www.maajournal.com

Mediterranean Archaeology and Archaeometry
Vol. 21, No 2, (2021), pp. 93-105
Open Access. Online & Print.

DOI: 10.5281/zenodo.4681734

APPLICATION OF FTIR SPECTROSCOPY TO THE CHARACTERIZATION OF WATERLOGGED ARCHAEOLOGICAL WOODS OF THREE GALLEYS FROM YENİKAPI, İSTANBUL: CONTRIBUTION TO CONSERVATION

A. Gökçe Kılıç*[1] and Namık Kılıç[2]

[1] Istanbul University Faculty of Letters Museology Department, Vezneciler, İstanbul, Turkey
[2] Istanbul University Faculty of Letters Department of Conservation of Marine Archaeological Objects, Laleli, İstanbul, Turkey

Received: 30/03/2021
Accepted: 12/04/2021
**Corresponding author: A. Gökçe Kılıç (gokcegokcay@istanbul.edu.tr)*

ABSTRACT

Thirty-seven shipwrecks, which are dated from 5th to 11th centuries AD, were uncovered under the supervision of the Istanbul Archaeology Museums Directorate in Yenikapı salvage excavations at Yenikapı, İstanbul. The woods of the Yenikapı shipwrecks, which were found during the excavation, were in the waterlogged state. The physical and chemical degradation degree of the waterlogged archaeological wood has been evaluated in detail to establish a successful conservation procedure. The determination of the chemical changes in the structure of the waterlogged archaeological wood provided information about the degradation process. In this study, fourteen untreated wood samples were taken from the three galleys of Yenikapı Shipwrecks (YK 13, YK 16, and YK 25), which are dated between the 7th and 10th centuries AD. In order to determine the chemical characterization of the waterlogged archaeological wood, the ATR-FTIR method was used. With the aim of making a safe comparison, three fresh wood samples (plane, pine, and elm) were also analysed. The spectral comparison all the changes of holocellulose and lignin components in the structure of the waterlogged archaeological wood samples were detected; the lignin degraded but it remained more intact than polysaccharides. New and additional data have been provided regarding the characterization of waterlogged archaeological woods for many ships in the Yenikapı Shipwrecks Project, the variety of the wood types used in the construction of the ships, and the usage of the ships such as galleys.

KEYWORDS: ATR-FTIR, degradation degree of waterlogged wood, holocellulose, lignin, Yenikapı shipwrecks.

1. INTRODUCTION

37 shipwrecks were uncovered under the supervision of the Istanbul Archaeology Museums Directorate in Yenikapı salvage excavations between the years 2004-2013. These shipwrecks are considered as the world's largest medieval shipwreck collection (Fig. 1). Furthermore, the six of these shipwrecks, which were the rowing ships, are also called galleys particularly important for being the first archaeological evidence of the galleys. The conservation work on 4 of these 6 galleys has been implemented by the Istanbul University's Department of Conservation of Marine Archaeological Objects (Totally 31 shipwrecks' conservation work has been implemented by the aforementioned department) (Kocabaş et al., 2012; Kocabaş, 2015; Akkemik and Kocabaş, 2013).

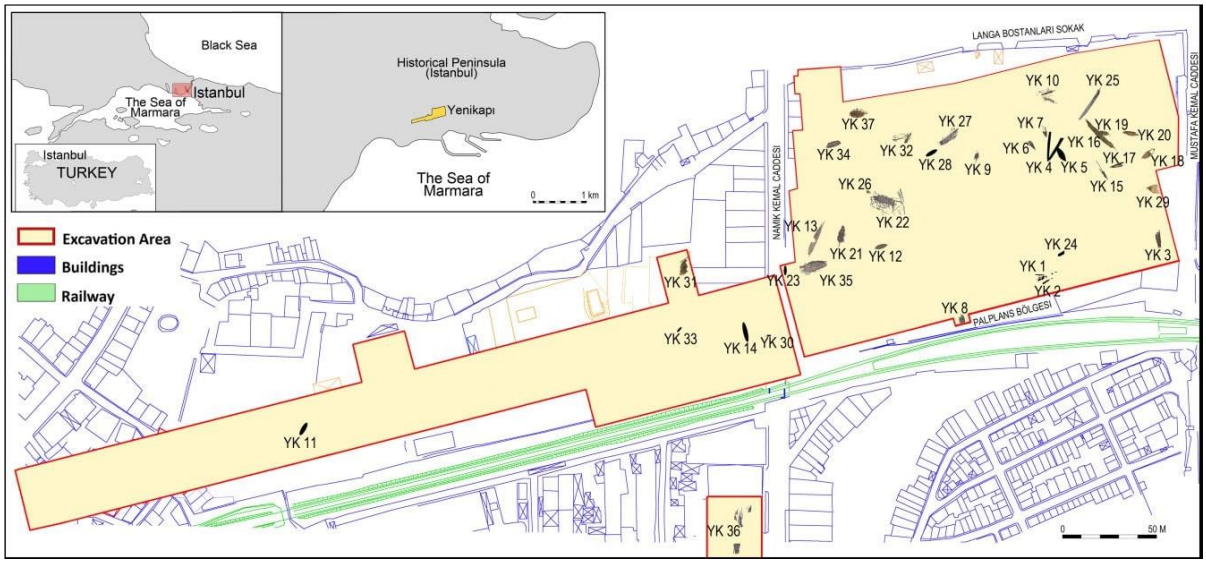

Figure 1. Distribution of wrecks across the excavation site (Kocabaş, 2015).

The shipwrecks uncovered in Yenikapı consisted of waterlogged archaeological woods. The waterlogged archaeological wood is filled with water and there is little or no air in cellular spaces, capillaries, and micro-capillaries of the woods (Rodgers, 2004; Antonelli et al, 2020). When it is wet, the waterlogged archaeological wood usually looks relatively in a good condition at the first sight. On the other hand, its physical, chemical, and mechanical properties degrade, and it changes into a spongy substance filled with water. Principally, the wood can remain intact in underwater environments where the microbial and fungal activities are limited but some of the bacteria can degrade the wood even in anaerobic conditions. This degradation causes a depletion of cellulose, hemicellulose, and lignin alteration. As a result, the density of the wood decreases, and the porosity and permeability of the wood increase (Broda et al., 2015; Coradeschi et al., 2018; Pizzo et al., 2010b).

In order to establish a successful conservation procedure, the physical and chemical conditions of the waterlogged archaeological wood should be evaluated in detail. In order to determine the physical condition of the waterlogged wood, several techniques, which are based on the correlation between the amount of water inside the wood and the loss of wood substance, are used, such as maximum water content (MWC), basic density, and loss of wood substance calculations (Brunning and Watson, 2010; Broda and Frankowski, 2017; Broda and Mazella, 2017; High and Penkman, 2020; Jensen and Gregory, 2006; Macchioni et al., 2018; Babiński et al., 2014; Macchioni et al., 2012; Kılıç, 2016; Kılıç and Kılıç, 2019a; Han et al., 2020a). The advantages of using these methods to determine the physical condition of the waterlogged archaeological wood are simplicity and cost efficiency. On the other hand, the results of these analyses do not give information on the degradation of the chemical compounds of the waterlogged archaeological wood. The chemical compounds of the wood are cellulose, hemicellulose, and lignin. Cellulose is a homopolymer. Hemicellulose is a carbohydrate heteropolymer. Lignin is an irregular, cross-linked polymer. In common, chemical analyses of waterlogged archaeological wood showed that the cellulose content of the waterlogged archaeological wood decreases, while the lignin content does not change extremely. On the other hand, the degradation process of the anaerobic erosion bacteria can cause an increase in the cellulose and hemicellulose contents in the waterlogged archaeological wood. Meanwhile, lignin can be degraded. Thus, the chemical characterization of the waterlogged archaeological wood is essential for the deter-

mination of the degradation processes of the waterlogged archaeological wood (Salanti et al., 2010; Björdal and Nilsson, 2002).

The traditional wet chemical analysis can be used to determine the degradation of the chemical compounds of the waterlogged archaeological wood. In order to determine the cellulose, the Seifert procedure can be applied. For the determination of the holocellulose, the Browning procedure can be applied. The lignin content can be determined according to the TAPPI standard (Broda et al, 2015; Capretti et al., 2008). The various components need to be separated in the traditional wet chemical analysis, although selective isolation of the wood subtracts is not easy (Łucejko et al., 2012). The main difficulty of the gravimetric analysis on waterlogged archaeological wood is getting accurate results on small samples (Ogilvie, 2000).

Analytical instrumental analysis techniques are used for the chemical characterization of waterlogged archaeological wood. X-ray diffraction (XRD) can be used for the determination of the degree of crystallinity of cellulose in waterlogged archaeological wood. In order to determine the molecular weight distribution of lignin, gel permeation chromatography (GPC) analysis can be performed. Quantitative evaluation of methoxy groups in lignin can be studied by using gas chromatography with a flame ionization detector (GC-FID). ^{13}C NMR can be used for the examination of celluloses and lignin in waterlogged archaeological wood. Fourier transform infrared (FTIR) spectroscopy can be used for analysing the holocellulose and lignin of the waterlogged archaeological wood (Łucejko et al., 2015; High and Penkman, 2020; Liritzis et al., 2020). FTIR is a useful and rapid technique which is used for chemical characterization of waterlogged archaeological wood. In addition, the use of the attenuated total reflection (ATR) attachment permits direct measurements on a solid sample without a sample preparation. Another advantage of this technique is the sufficiency of performing the analysis with a very small sample (Kazarian and Chan, 2016; Akyüz, 2018). ATR-FTIR analyses were conducted on many waterlogged archaeological wood samples from various countries. The samples from Denmark were analysed by ATR-FTIR (Christensen et al., 2006; Eriksen et al., 2015). The samples from the EU-project BACPOLES of 27 sample sites in Europe were examined with the ATR-FTIR method to determine the lignin content of the samples (Gelbrich et al., 2008; Gelbrich et al., 2012). ATR-FTIR analyses were performed on the samples coming from several excavations carried out in Italy (Pizzo et al., 2010a; Pizzo et al 2013¸ Pizzo et al., 2015). The archaeological wood samples, which were originated from a shipwreck and from a beam wood of a cathedral in Spain, were analysed by ATR-FTIR (Traoré et al, 2016). Waterlogged wood finds from the Dead Sea were investigated with ATR-FTIR (Oron et al., 2016). The samples, which were collected from waterlogged archaeological wood Xiaobaijiao No. 1 shipwreck, were studied with ATR-FTIR (Han et al., 2020b). In addition to these studies, the different samples taken from Yenikapı shipwrecks were analysed by ATR-FTIR method (Kılıç and Kılıç, 2019b). The scientific studies conducted in the Yenikapı Shipwrecks Project provided new data for the conservation of the waterlogged archaeological wood by reason of the large number of ships in the project, the variety of the wood types used in the construction of the ships, and the different purposes of using the ships, such as rowing ships and trade ships. This study focused on the application of FTIR spectroscopy to the characterization of waterlogged archaeological woods of three galleys from Yenikapı Shipwrecks.

This study focused on 3 galleys which were found at Yenikapı during salvage excavations: YK 13, YK 16, and YK 25. The chemical composition of the waterlogged archaeological woods taken from 3 galleys was examined by using the ATR-FTIR method.

2. MATERIALS AND METHODS

2.1 Sampling

The study was done on 14 waterlogged archaeological wood samples taken from 3 galleys found at Yenikapı in İstanbul. The first of these galleys was YK 13. It is dated to 690-890 AD by radiocarbon analyses and its extant length is 20.8 m and width 2.8 m. The other galley, which was renamed as YK 16, is dated to 720–890 AD by radiocarbon analyses and its extant length is 22.5 m and width 2.4 m. Finally, the third galley, which was renamed as YK 25, is dated to the 10th century by its stratigraphic context and its extant length is 19 m and width 1.5 m (Fig. 2). The main tree species used in the construction of these galleys are plane (*Platanus L.*), elm (*Ulmus L.*), and pine (*Pinus L.*). All wood identification process was performed by Prof. Dr. Ünal Akkemik from Wood Anatomy Laboratory of the Department of Forest Botany, Faculty of Forestry, Istanbul University- Cerrahpaşa. Three sections cross, tangential and radial sections, from each wood sample were taken and a reference collection at the laboratory and wood anatomical references were used for identification (Kocabaş, 2012; Kocabaş, 2015; Akkemik and Kocabaş, 2013; Akkemik, 2015). Tree species of the waterlogged archaeological wood samples were given in Table 1.

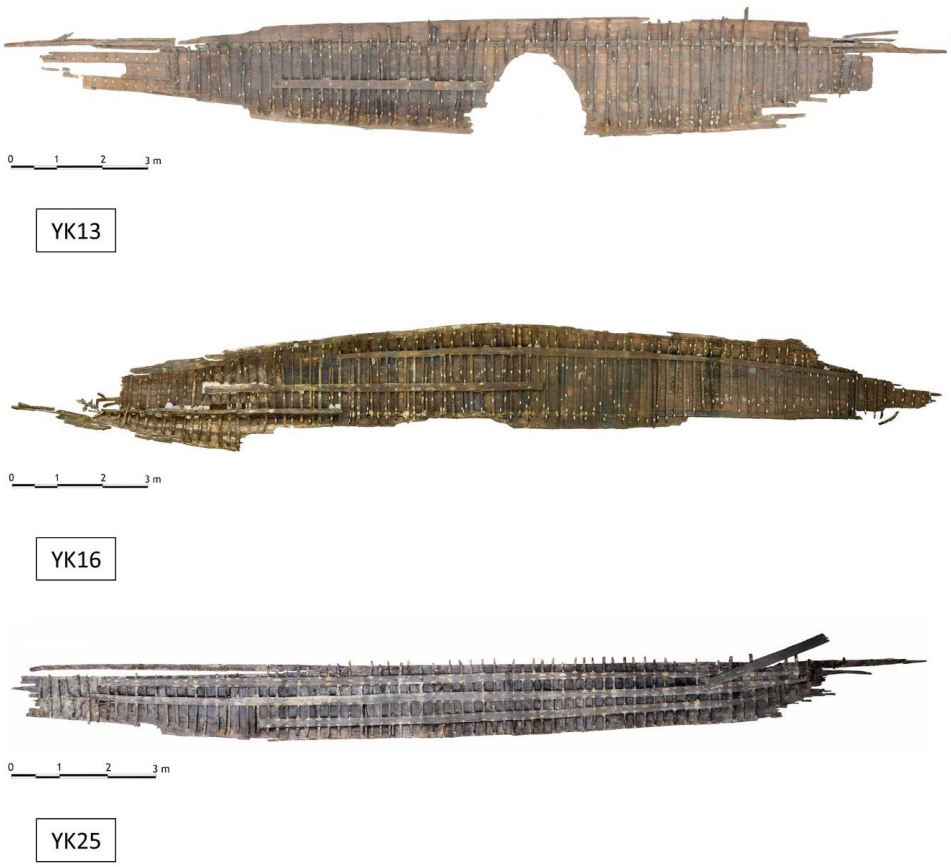

Figure 2. Photos of the shipwrecks (IU Yenikapı Shipwrecks Project Archive).

All of the samples were taken from the woods which were kept in desalination tanks, and all of them were untreated. In addition, plane, pine, and elm fresh wood samples were taken for ATR-FTIR analyses to compare the spectrum of the waterlogged archaeological wood sample to the spectrum of the fresh wood sample. The wood samples were prepared as thin sections and the diameter of them was approximately 4 mm. Waterlogged archaeological wood samples and fresh wood samples were dried in an oven before performing the ATR-FTIR analysis in order to prevent error in the results due to water.

Table 1. Tree species of the waterlogged archaeological wood samples.

The Shipwreck Name	Sample	Species
YK 13	IB1-1	Pine *(Pinus L.)*
YK13	IK2-1	Pine *(Pinus L.)*
YK16	E77	Elm tree (*Ulmus L.)*
YK16	E115-S1	Elm tree (*Ulmus L.)*
YK16	S-E48	Elm tree (*Ulmus L.)*
YK 25	E4-I1	Plane *(Platanus L.)*
YK 25	E15	Plane *(Platanus L.)*
YK 25	E16	Plane *(Platanus L.)*
YK 25	E31	Plane *(Platanus L.)*
YK 25	E32	Plane *(Platanus L.)*
YK 25	E33	Plane *(Platanus L.)*
YK 25	E35	Plane *(Platanus L.)*
YK 25	E38	Plane *(Platanus L.)*
YK 25	IB1-2	Pine *(Pinus L.)*

Key to symbols
E: Frame,
IB: Portside garboard,
IK: Portside planking,
S: Starboard.

2.2. *ATR-FTIR analyses*

FTIR spectroscopy was carried out on a Perkin Elmer Spectrum One series FTIR spectrometer using an attenuation total reflection (ATR) sampling accessory. The study was performed on an archaeological material therefore ATR sampling accessory was used to analyse very small samples. All the spectra were acquired (16 scans/sample) in the range of 4000 – 600 cm^{-1} at a Fourier transform (FT) resolution of 4 cm^{-1} and subsequently had a ratio against a 16-scan open-beam background spectrum to produce absorbance. The FTIR spectra of the wood samples were baseline corrected in Spectrum One. The spectra were recorded as absorbance versus wavenumber. The data evaluation was limited to the fingerprint region of the wood (1800–800 cm^{-1}) (Fors et al., 2011).

3. RESULTS AND DISCUSSION

Fourteen waterlogged archaeological wood samples and three fresh wood samples were analysed with the ATR-FTIR method. In order to determine the chemical degradation of the waterlogged archaeological wood samples, the spectrum of the waterlogged archaeological wood sample and the spectrum of the fresh wood sample were compared. With the aim of making a healthy comparison, the spectra of the same wood species were compared. The species of the wood samples, which were analysed in this study, are plane, pine, and elm woods. Eight plane waterlogged archaeological wood samples, three pine waterlogged archaeological wood samples, and three elm waterlogged archaeological wood samples were analysed in this study. Firstly, the FTIR spectra of fresh plane wood and waterlogged plane wood samples were analysed (Fig. 3).

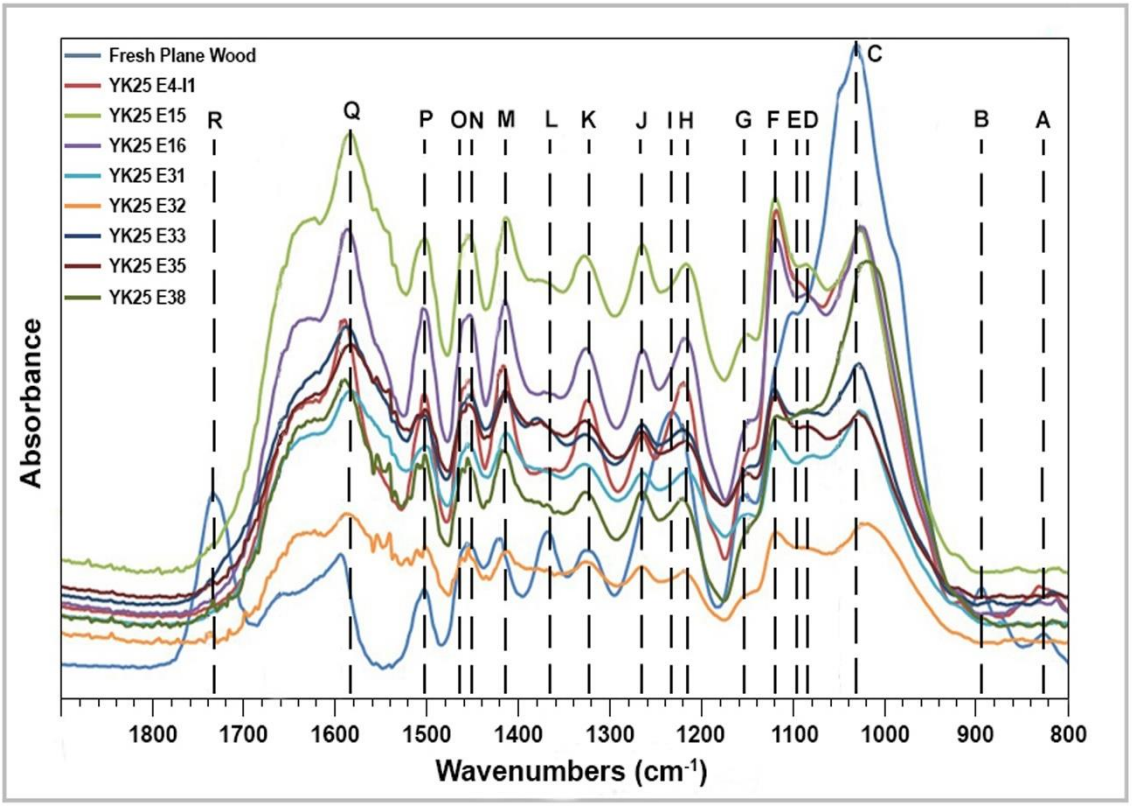

Figure 3. The FTIR spectra of the fresh plane wood and the waterlogged plane wood samples.

When all the spectra in Fig. 3 were examined, the changes of cellulose, hemicellulose and lignin components in the structure of the waterlogged archaeological wood samples were detected (Cesar et al., 2017). The band at ~ 825 cm^{-1} (the peaks were shown on the spectra as A with dotted lines) was related to lignin (Traoré et al., 2018). This peak was detected in the spectrum of the fresh plane wood sample. On the other hand, the intensity of this peak decreased or there was no peak on the spectra of the waterlogged plane wood samples. The band at ~ 896 cm^{-1} (the peaks were shown on the spectra as B with dotted lines) was associated with stretching and bending vibration of molecular bonds of the cellulose (Hospodarova et al., 2018). This peak was detected in the spectrum of the fresh plane wood sample. On the other hand, the intensity of this peak decreased or there was no peak in the spectra of the waterlogged plane wood samples. The band at ~ 1030 cm^{-1} (the peaks were shown on the spectra as C with dotted

lines) belonged to the C–O stretch in cellulose and hemicellulose (Naumann et al., 2007). This peak was detected in the spectrum of the fresh plane wood sample. On the other hand, the intensity of this peak decreased in the spectra of the waterlogged plane wood samples. The band at ~ 1086 cm^{-1} (the peaks were shown on the spectra as D with dotted lines) was related to lignin degradation (Rashid et al., 2016) This peak was detected in the spectra of the some of the waterlogged plane wood samples. On the other hand, there was no peak in the spectrum of the fresh plane wood sample. The band at ~ 1105 cm^{-1} (the peaks were shown on the spectra as E with dotted lines) was associated with carbohydrate (McLean et al., 2014). This peak was detected in the spectrum of the fresh plane wood sample. On the other hand, there was no peak in the spectra of the waterlogged plane wood samples. The band at ~ 1126 cm^{-1} (the peaks were shown on the spectra as F with dotted lines) was linked with the degradation of the lignin (Pucetaite 2012). This peak was detected in the spectra of the waterlogged plane wood samples. On the other hand, there was no peak of the fresh plane wood sample. The band at ~ 1155 cm^{-1} (the peaks were shown on the spectra as G with dotted lines) belonged to C–O vibration in cellulose and hemicellulose (Naumann et al., 2007). This peak was detected in the spectrum of the fresh plane wood sample. On the other hand, the intensity of this peak decreased in the spectra of the waterlogged plane wood samples. The band at ~ 1216 cm^{-1} (the peaks were shown on the spectra as H with dotted lines) indicated an esterification of the wood (Giridgar et al., 2017). This peak was detected in the spectra of the waterlogged plane wood samples. On the other hand, there was no peak in the spectrum of the fresh plane wood sample. The band at ~ 1235 cm^{-1} (the peaks were shown on the spectra as I with dotted lines) was associated with the syringyl ring and the C= stretch in lignin and xylan (Müller et al., 2009). This peak was detected in the spectrum of the fresh plane wood sample. On the other hand, there was no peak in the spectra of the waterlogged plane wood samples. The band at ~ 1265 cm^{-1} (the peaks were shown on the spectra as J with dotted lines) was related to syringyl ring breathing and C-O stretching vibration in lignin and xylan (Shi et al., 2012). This peak was detected in the spectra of the waterlogged plane wood samples. On the other hand, there was no peak in the spectrum of the fresh plane wood sample. The band at ~ 1326 cm^{-1} (the peaks were shown on the spectra as K with dotted lines) was associated with C–O vibration in syringyl rings and C–H bonds in cellulose (Traoré et al., 2016). This peak was detected in all spectra. The band at ~ 1367 cm^{-1} (the peaks were shown on the spectra as L with dotted lines) was related to cellulose (Hospodarova et al., 2018). This peak was detected in the spectrum of the fresh plane wood sample. On the other hand, there was no peak in the spectra of the waterlogged plane wood samples. The band at ~ 1420 cm^{-1} (the peaks were shown on the spectra as M with dotted lines) was related to the amount of the crystalline structure of the cellulose (Hospodarova et al., 2018). This peak was detected in all spectra. The band at ~ 1456 cm^{-1} (the peaks were shown on the spectra as N with dotted lines) was associated with lignin (Fackler et al., 2010). This peak was detected in all spectra. The band at ~ 1460 cm^{-1} (the peaks were shown on the spectra as O with dotted lines) was related to lignin (Moosavinejad et al., 2019). This peak was detected in all spectra. The band at ~ 1502 cm^{-1} (the peaks were shown on the spectra as P with dotted lines) was associated with lignin (Pandey, 1999). This peak was detected in all spectra. The band at ~ 1592 cm^{-1} (the peaks were shown on the spectra as Q with dotted lines) belonged to lignin (Zborowska et al., 2016). This peak was detected in all spectra. The band at ~ 1732 cm^{-1} (the peaks were shown on the spectra as R with dotted lines) was associated with unconjugated carbonyl stretching in hemicelluloses (Kubovský et al., 2020). This peak was detected in the spectrum of the fresh plane wood sample. On the other hand, the intensity of this peak decreased or there was no peak in the spectra of the waterlogged plane wood samples.

The FTIR measurements of the plane wood samples were made first, followed by those of fresh pine wood and waterlogged pine wood samples (Fig. 4).

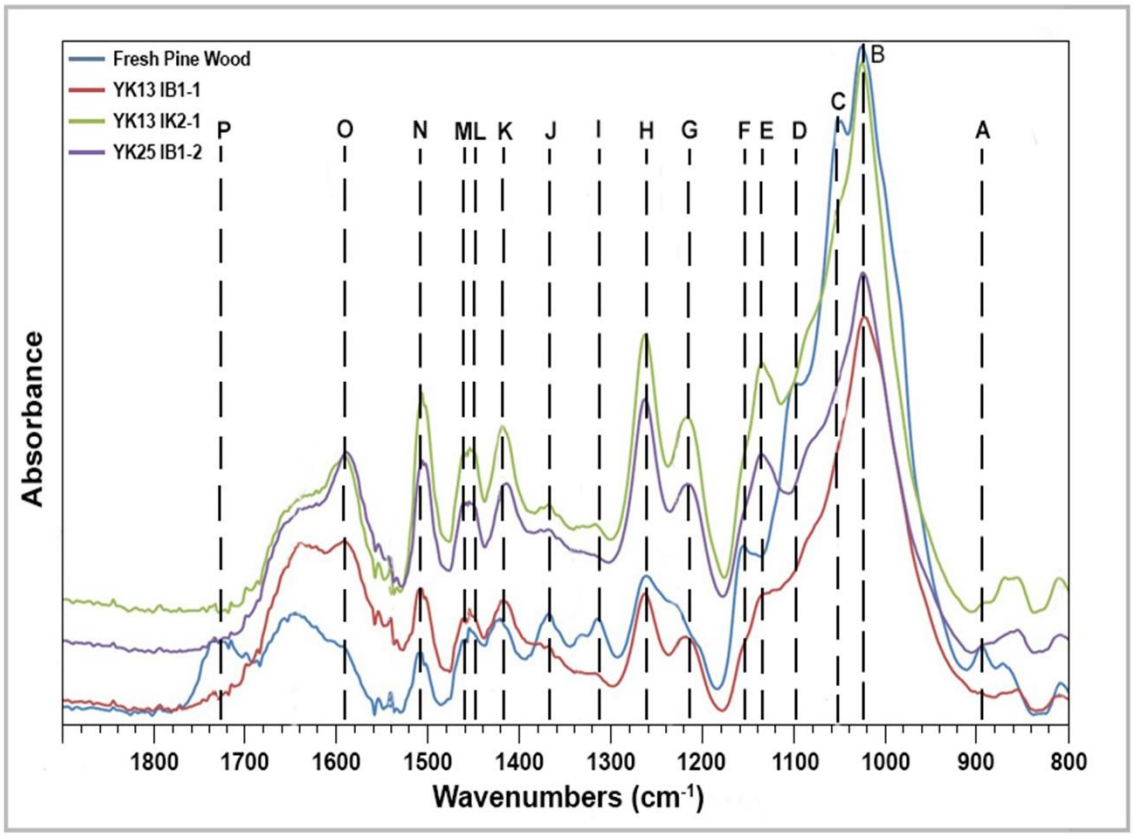

Figure 4. The FTIR spectra of the fresh pine wood and the waterlogged pine wood samples.

When all the spectra in Fig. 4 were examined, sixteen peaks could be detected. The band at ~ 898 cm^{-1} (the peaks were shown on the spectra as A with dotted lines) was associated with carbohydrate (Pandey and Pitman, 2003). This peak was detected in the spectrum of the fresh pine wood sample. On the other hand, the intensity of this peak decreased or there was no peak in the spectra of the waterlogged pine wood samples. The band at ~ 1030 cm^{-1} (the peaks were shown on the spectra as B with dotted lines) belonged to C–O stretch in cellulose and hemicellulose (Naumann et al., 2007). This peak was detected in the spectra of all samples. The band at ~ 1044 cm^{-1} (the peaks were shown on the spectra as C with dotted lines) was related to carbohydrate (Pucetaite, 2012). This peak was detected in the spectra of the waterlogged pine wood samples. On the other hand, there was no peak in the spectrum of the fresh pine wood sample. The band at ~ 1105 cm^{-1} (the peaks were shown on the spectra as D with dotted lines) was associated with carbohydrate (Pandey and Pitman, 2003). This peak was detected in the spectrum of the fresh pine wood sample. On the other hand, there was no peak in the spectra of the waterlogged pine wood samples. The band at ~ 1140 cm^{-1} (the peaks were shown on the spectra as E with dotted lines) was related to C–H deformation in aromatic rings (Esteves et al., 2013). This peak was detected in the spectra of the waterlogged pine wood samples. On the other hand, there was no peak in the spectrum of the fresh pine wood sample. The band at ~ 1164 cm^{-1} (the peaks were shown on the spectra as F with dotted lines) indicated polysaccharides (Viet, 2017). This peak was detected in the spectrum of the fresh pine wood sample. On the other hand, there was no peak in the spectra of the waterlogged pine wood samples. The band at ~ 1216 cm^{-1} (the peaks were shown on the spectra as G with dotted lines) indicated esterification of the wood (Giridhar et al., 2017). This peak was detected in the spectra of the waterlogged pine wood samples. On the other hand, there was no peak in the spectrum of the fresh pine wood sample. The band at ~ 1265 cm^{-1} (the peaks were shown on the spectra as H with dotted lines) was related to syringyl ring breathing and C-O stretching vibration in lignin and xylan (Shi et al., 2012). This peak was detected in the spectra of all samples. The band at ~ 1316 cm^{-1} (the peaks were shown on the spectra as I with dotted lines) was associated with cellulose (Stevanic and Salmén, 2009). This peak was detected in the spectrum of the fresh pine wood sample. On the other hand, the intensity of this peak decreased or there was no peak in the spectra of the waterlogged pine wood samples. The band at ~ 1367 cm^{-1} (the peaks were shown on the spectra as J with dotted lines) was related to cellulose (Hospodarova et al., 2018). This peak was detected in the

spectrum of the fresh pine wood sample. On the other hand, the intensity of this peak decreased in the spectra of the waterlogged pine wood samples. The band at ~ 1420 cm^{-1} (the peaks were shown on the spectra as K with dotted lines) was related to the amount of the crystalline structure of the cellulose (Hospodarova et al., 2018). This peak was detected in all spectra. The band at ~ 1456 cm^{-1} (the peaks were shown on the spectra as L with dotted lines) was associated with lignin (Fackler et al., 2010). This peak was detected in all spectra. The band at ~ 1460 cm^{-1} (the peaks were shown on the spectra as M with dotted lines) was related to lignin (Moosavinejad et al., 2019). This peak was detected in all spectra. The band at ~ 1502 cm^{-1} (the peaks were shown on the spectra as N with dotted lines) was associated with lignin (Pandey, 1999). This peak was detected in all spectra. The band at ~ 1592 cm^{-1} (the peaks were shown on the spectra as O with dotted lines) belonged to lignin (Zborowska et al., 2016). This peak was detected in all spectra. The band at ~ 1732 cm^{-1} (the peaks were shown on the spectra as P with dotted lines) was associated with unconjugated carbonyl stretching in hemicelluloses (Kubovský et al., 2020). This peak was detected in the spectrum of the fresh pine wood sample. On the other hand, there was no peak in the spectra of the waterlogged pine wood samples.

Finally, the FTIR spectra of the fresh elm wood and the waterlogged elm wood samples were analysed (Fig. 5).

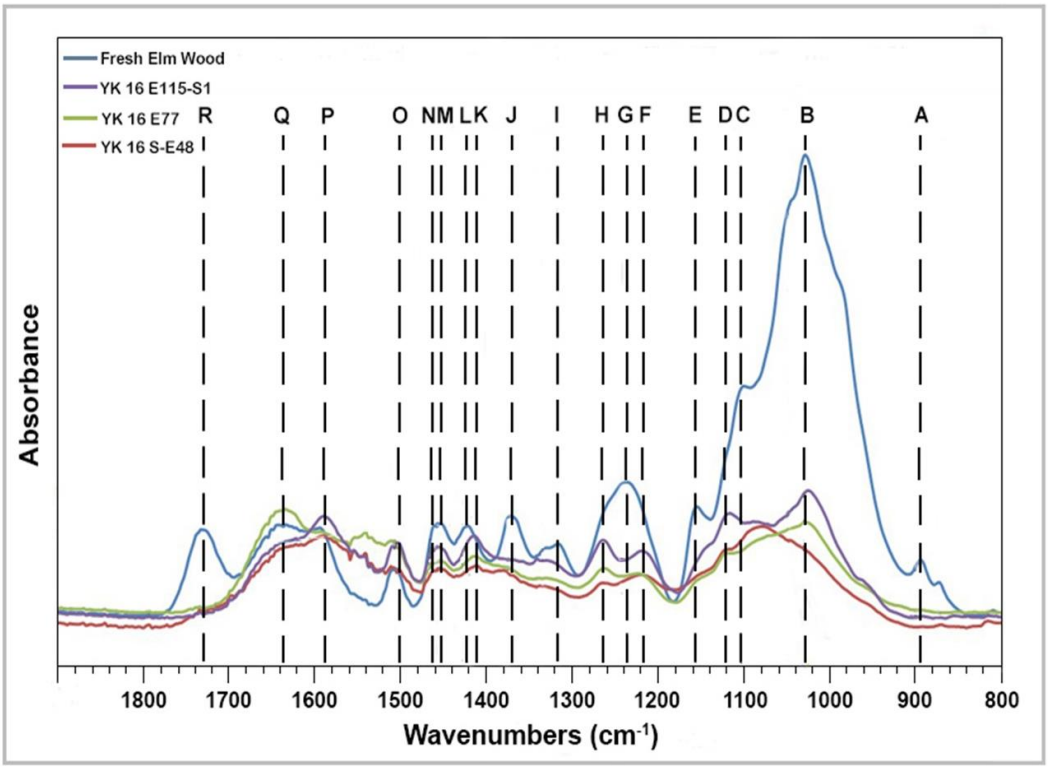

Figure 5. The FTIR spectra of the fresh elm wood and the waterlogged elm wood samples.

When all the spectra in Fig. 5 were examined, eighteen peaks could be detected. The band at ~ 896 cm^{-1} (the peaks were shown on the spectra as A with dotted lines) was associated with stretching and bending vibration of molecular bonds of the cellulose cellulose (Hospodarova et al., 2018). This peak was detected in the spectrum of the fresh elm wood sample. On the other hand, there was no peak in the spectra of the waterlogged elm wood samples. The band at ~ 1030 cm^{-1} (the peaks were shown on the spectra as B with dotted lines) belonged to C–O stretch in cellulose and hemicellulose (Naumann et al., 2007). This peak was detected in the spectrum of the fresh elm wood sample. On the other hand, the intensity of this peak decreased or there was no peak in the spectra of the waterlogged elm wood samples. The band at ~ 1105 cm^{-1} (the peaks were shown on the spectra as C with dotted lines) was associated with carbohydrate (McLean et al., 2014). This peak was detected in the spectrum of the fresh elm wood sample. On the other hand, there was no peak in the spectra of the waterlogged elm wood samples. The band at ~ 1140 cm^{-1} (the peaks were shown on the spectra as D with dotted lines) was related to C–H deformation in aromatic rings (Esteves et al., 2013). This peak was detected in the spectra of the waterlogged elm wood samples. On the other hand, there was no peak in the spectrum of the fresh elm wood sample. The band at ~ 1155 cm^{-1} (the peaks were shown on the spectra as E with dotted

lines) belonged to C–O vibration in cellulose and hemicellulose (Naumann et al., 2007). This peak was detected in the spectrum of the fresh elm wood sample. On the other hand, there was no peak in the spectra of the waterlogged elm wood samples. The band at ~ 1216 cm^{-1} (the peaks were shown on the spectra as F with dotted lines) indicated esterification of the wood (Giridhar et al., 2017). This peak was detected in the spectra of the waterlogged elm wood samples. On the other hand, there was no peak in the spectrum of the fresh elm wood sample. The band at ~ 1235 cm^{-1} (the peaks were shown on the spectra as G with dotted lines) was associated with syringyl ring and C= stretch in lignin and xylan (Müller et al., 2009). This peak was detected in the spectrum of the fresh elm wood sample. On the other hand, there was no peak in the spectra of the waterlogged elm wood samples. The band at ~ 1265 cm^{-1} (the peaks were shown on the spectra as H with dotted lines) was related to syringyl ring breathing and C-O stretching vibration in lignin and xylan (Shi et al., 2012). This peak was detected in the spectra of the waterlogged elm wood samples. On the other hand, there was no peak in the spectrum of the fresh elm wood sample. The band at ~ 1316 cm^{-1} (the peaks were shown on the spectra as I with dotted lines) was associated with cellulose (Stevanic and Salmén, 2009). This peak was detected in the spectrum of the fresh elm wood sample. On the other hand, there was no peak in the spectra of the waterlogged elm wood samples. The band at ~ 1367 cm^{-1} (the peaks were shown on the spectra as J with dotted lines) was related to cellulose cellulose (Hospodarova et al., 2018). This peak was detected in the spectrum of the fresh elm wood sample. On the other hand, there was no peak in the spectra of the waterlogged elm wood samples. The band at ~ 1412 cm^{-1} (the peaks were shown on the spectra as K with dotted lines) was related to C–H deformation (Shearer, 1990). This peak was detected in the spectra of the waterlogged elm wood sample. On the other hand, there was no peak in the spectrum of the fresh elm wood sample. The band at ~ 1420 cm^{-1} (the peaks were shown on the spectra as L with dotted lines) was related to the amount of the crystalline structure of the cellulose cellulose (Hospodarova et al., 2018). This peak was detected in the spectrum of the fresh elm wood sample. On the other hand, there was no peak in the spectra of the waterlogged elm wood samples. The band at ~ 1456 cm^{-1} (the peaks were shown on the spectra as M with dotted lines) was associated with lignin (Fackler et al., 2010). This peak was detected in all spectra. The band at ~ 1460 cm^{-1} (the peaks were shown on the spectra as N with dotted lines) was related to lignin (Moosavinejad et al., 2019). This peak was detected in all spectra. The band at ~ 1502 cm^{-1} (the peaks were shown on the spectra as O with dotted lines) was associated with lignin (Pandey, 1999). This peak was detected in all spectra. The band at ~ 1592 cm^{-1} (the peaks were shown on the spectra as P with dotted lines) belonged to lignin (Zborowska et al., 2016). This peak was detected in all spectra. The band at ~ 1654 cm^{-1} (the peaks were shown on the spectra as Q with dotted lines) was related to lignin (Moosavinejad et al., 2019). This peak was detected in the spectrum of the fresh elm wood sample. On the other hand, the intensity of this peak decreased or there was no peak in the spectra of the waterlogged elm wood samples. The band at ~ 1732 cm^{-1} (the peaks were shown on the spectra as R with dotted lines) was associated with unconjugated carbonyl stretching in hemicelluloses (Kubovský et al., 2020). This peak was detected in the spectrum of the fresh elm wood sample. On the other hand, there was no peak in the spectra of the waterlogged elm wood samples.

When Figures 3, 4, and 5 were examined, it was understood that the bands at ~ 1030, 1105, 1265, 1367, 1420, 1456, 1460, 1502, 1592, and 1732 cm^{-1} were found in all figures. These bands were associated with chemical components of the wood such as cellulose, hemicellulose, and lignin. Besides these bands, the band at ~ 1216 cm^{-1} was also found in all spectra except spectra of the fresh wood samples and this band was related to the degradation of the chemical structure of the wood.

Finally, in the spectra of the fresh wood samples, the bands at ~ 1235 and 1265 cm^{-1} appeared as one broad peak. On the other hand, the degradation of lignin resulted in the separation of these two peaks in the spectra of waterlogged archaeological wood (High and Penkman, 2020).

When all data was examined, it was concluded that lignin remained more intact than polysaccharides. Especially, hemicellulose could be affected by hydrolysis (Almkvist, 2008), and lignin was degraded. Enzymatic oxidation of the lignin caused by biological activities under anaerobic conditions was a reason for the degradation. In addition, an increased concentration of the more resistant Guaiacyl lignin was more resistant than Syringyl lignin in the waterlogged archaeological wood (High and Penkman, 2020). These results were consistent with the results of the previous studies in the conservation of the waterlogged archaeological wood. Thus, different molecular weight conservation chemicals can be used according to the degradation status of the waterlogged wood. For polyethylene glycol (PEG) impregnation, high molecular weight PEG can be used for the conservation of highly degraded waterlogged woods and low molecular weight PEG can be used for well-preserved waterlogged wood.

4. CONCLUSION

Due to the large number of ships in the Yenikapı Shipwrecks Project, the variety of the wood types used in the construction of the ships and the different purposes for using the ships, the scientific studies, which were conducted in the project, provided important data for the conservation of the waterlogged archaeological wood. The degradation of the chemical structure of the waterlogged archaeological wood samples, which were taken from the three galleys of the Yenikapı Shipwrecks, were examined in this study. All the samples were taken from untreated woods in order to compare the spectrum of the waterlogged archaeological wood sample to the spectrum of the fresh wood sample easily. The bands which were caused by conservation chemicals could be concealed by the bands of the wood samples. The degradation of the cellulose, hemicellulose, and lignin was reflected by the spectroscopic data which were acquired by the ATR-FTIR method. It was found that lignin remained more intact than cellulose and hemicellulose. It was determined that lignin degraded due to biological activities under anaerobic conditions. With these data, the degradation status of the chemical components of the waterlogged wood samples and their degradation reasons were identified. This information of the degradation status of the waterlogged wood, helps for an appropriate conservation chemical be chosen for the impregnation process of the waterlogged wood.

ACKNOWLEDGMENTS

We would like to acknowledge Prof. Dr. Ufuk Kocabaş, Istanbul Archaeology Museums, and Yenikapı Shipwrecks Project Team for their help and support. The IU Yenikapı Shipwrecks Project has been realized with the financial support of İstanbul University Scientific Research Projects Unit (Project nos: 2294, 3907, 7381, 12765, SDK-2016-3777, SDK-2016-3776).

REFERENCES

Akkemik, Ü. (2015) Woods of Yenikapi Shipwrecks. Ege Yayınları, Istanbul.

Akkemik, Ü. and Kocabaş, U. (2013) Woods of the old galleys of Yenikapi, Istanbul. *Mediterranean Archaeology & Archaeometry* 13.2, pp. 31-41.

Akyüz, S. (2018) Investigation of the degradation stages of archaeological and historic silk textiles: An ATR-FTIR spectroscopic study. *Archaeology Anthropology: Open Access* 3-1, pp. 447-451.

Almkvist, G. (2008) The Chemistry of the Vasa. Doctoral dissertation, Swedish University of Agricultural Sciences.

Antonelli, F., Esposito, A., Galotta, G., Davidde Petriaggi, B., Piazza, S., Romagnoli, M. and Guerrieri, F. (2020) Microbiota in waterlogged archaeological wood: Use of Next-Generation Sequencing to evaluate the risk of biodegradation. *Applied Sciences*, 10(13), 4636

Babiński, L., Izdebska-Mucha, D. and Waliszewska, B. (2014) Evaluation of the state of preservation of waterlogged archaeological wood based on its physical properties: basic density vs. wood substance density. J*ournal of Archaeological Science* 46, pp. 372–383.

Björdal, C. G. and Nilsson, T. (2002) Waterlogged archaeological wood—a substrate for white rot fungi during drainage of wetlands. *International biodeterioration & biodegradation* 50(1), pp. 17-23.

Broda, M. and Frankowski, M. (2017) Determination of the content of selected elements in medieval waterlogged oak wood from the Lednica Lake—a case study. *Environmental Science and Pollution Research* 24.29, pp. 23401-23410.

Broda, M. and Mazela, B. (2017) Application of methyltrimethoxysilane to increase dimensional stability of waterlogged wood. *Journal of Cultural Heritage* 25, pp. 149-156.

Broda, M., Mazela, B., Krolikowska-Pataraja, K. and Siuda, J. (2015) The state of degradation of waterlogged wood from different environments. Annals of Warsaw University of Life Sciences-SGGW. *Forestry and Wood Technology*, 91, pp. 23-27.

Brunning, R. and Watson, J. (2010) *Waterlogged wood: guidelines on the recording, sampling, conservation, and curation of waterlogged wood*. English Heritage.

Capretti, C., Macchioni, N., Pizzo, B., Galotta, G., Giachi, G. and Giampaola, D. (2008) The characterization of waterlogged archaeological wood: the three Roman ships found in Naples (Italy). *Archaeometry* 50(5), pp. 855-876.

Cesar, T., Danevčič, T., Kavkler, K. and Stopar, D. (2017) Melamine polymerization in organic solutions and waterlogged archaeological wood studied by FTIR spectroscopy. *Journal of Cultural Heritage* 23, pp. 106-110.

Christensen, M., Frosch, M., Jensen, P., Schnell, U., Shashoua, Y. and Nielsen, O. F. (2006) Waterlogged

archaeological wood—chemical changes by conservation and degradation. *Journal of Raman Spectroscopy* 37(10), pp. 1171-1178.

Coradeschi, G., Manhita, A., Dias, C.B., Mota, N., Caessa, A., Nozes, C., Sadori, L., Branco, F. and Gonçalves, L. (2018) Archaeometric study of waterlogged wood from the Roman cryptoporticus of Lisbon. Conserving Cultural Heritage: *Proceedings of the 3rd International Congress on Science and Technology for the Conservation of Cultural Heritage*. CRC Press, pp. 323-325.

Eriksen, A. M., Gregory, D. and Shashoua, Y. (2015) Selective attack of waterlogged archaeological wood by the shipworm, Teredo navalis and its implications for in-situ preservation. *Journal of Archaeological Science 55*, pp. 9-15.

Esteves, B., Velez Marques, A., Domingos, I. and Pereira, H. (2013) Chemical changes of heat treated pine and eucalypt wood monitored by FTIR. Maderas. *Ciencia y tecnología* 15(2), pp. 245-258.

Fackler, K., Stevanic, J.S., Ters, T., Hinterstoisser, B., Schwanninger, M. and Salmén, L. (2010) Localisation and characterisation of incipient brown-rot decay within spruce wood cell walls using FT-IR imaging microscopy. *Enzyme and microbial technology* 47(6), pp. 257-267.

Fors, Y., Jalilehvand, F. and Sandström, M. (2011) Analytical aspects of waterlogged wood in historical shipwrecks. *Analytical Sciences* 27(8), pp. 785-785.

Gelbrich, J., Mai, C. and Militz, H. (2008) Chemical changes in wood degraded by bacteria. *International Biodeterioration & Biodegradation* 61(1), pp. 24-32.

Gelbrich, J., Mai, C. and Militz, H. (2012) Evaluation of bacterial wood degradation by Fourier Transform Infrared (FTIR) measurements. *Journal of Cultural heritage* 13(3), pp. S135-S138.

Giridhar, N., Pandey, K. K., Prasad, B. E., Bisht, S. S. and Vagdevi, H. M. (2017) Dimensional stabilization of wood by chemical modification using isopropenyl acetate. Maderas. *Ciencia y tecnología* 19(1), pp. 15-20.

Han, L., Guo, J., Wang, K., Grönquist, P., Li, R., Tian, X. and Yin, Y. (2020a) Hygroscopicity of Waterlogged Archaeological Wood from Xiaobaijiao No. 1 Shipwreck Related to Its Deterioration State. *Polymers* 12(4), 834, pp.1-15.

Han, L., Tian, X., Keplinger, T., Zhou, H., Li, R., Svedström, K., Burgert, I., Yin, Y. and Guo, J. (2020b) Even visually intact cell walls in waterlogged archaeological wood are chemically deteriorated and mechanically fragile: a case of a 170 year-old shipwreck. *Molecules* 25(5), 1113.

High, K. E. and Penkman, K. E. (2020) A review of analytical methods for assessing preservation in waterlogged archaeological wood and their application in practice. *Heritage Science* 8(1), pp. 1-33.

Hospodarova, V., Singovszka, E., and Stevulova, N. (2018) Characterization of cellulosic fibers by FTIR spectroscopy for their further implementation to building materials. *American Journal of Analytical Chemistry* 9(6), pp. 303-310.

Jensen, P. and Gregory, D. J. (2006) Selected physical parameters to characterize the state of preservation of waterlogged archaeological wood: a practical guide for their determination. *Journal of Archaeological Science* 33(4), pp. 551–559.

Kazarian, S. G. and Chan, K. L. A. (2016) FTIR Imaging of Polymeric Materials. *Polymer Morphology: Principles, Characterization, and Processing*, pp.118-130.

Kılıç, N. (2016). Conservation of a Group of Frames from YK 16 Shipwreck (Yenikapı 16 Batığına Ait Bir Grup Eğrinin Konservasyonu). *Art-Sanat,* 6, pp. 85-97.

Kılıç, N., and Kılıç, A.G. (2019a) Physical properties for the characterization of waterlogged archaeological woods of eight Yenikapı shipwrecks from Byzantine period. *Mediterranean Archaeology & Archaeometry* 19(2), pp. 133-148.

Kılıç, N. and Kılıç, A. G. (2019b) An attenuated total reflection Fourier transform infrared (ATR-FTIR) spectroscopic study of waterlogged woods treated with melamine formaldehyde. *Vibrational Spectroscopy* 105, 102985.

Kocabaş, U. (2012). The Latest Link in the Long Tradition of Maritime Archaeology in Turkey: The Yenikapı Shipwrecks. *European Journal of Archaeology*, *15*(2), pp. 309-323.

Koçabaş, U., Özsait Kocabaş, I. and Kılıç, N. (2012). The Yenikapı Shipwrecks: Dismantling Methods and First Step to Conservation. *11th ICOM International Conference on Wet Organic Archaeological Materials (ICOM-WOAM),* Eds. Kristiane Straetkvern, Emily Williams, Istanbul, pp. 303-312.

Kocabaş, U. (2015) The Yenikapı Byzantine-Era Shipwrecks, Istanbul, Turkey: a preliminary report and inventory of the 27 wrecks studied by Istanbul University. *International Journal of Nautical Archaeology* 44.1, pp. 5-38.

Kubovský, I., Kačíková, D. and Kačík, F. (2020) Structural changes of oak wood main components caused by

thermal modification. *Polymers* 12(2), 485.
Liritzis, I.., Laskaris, N., Vafiadou, A., Karapanagiotis, I., Volonakis, P., Papageorgopoulou, C. and Bratitsi, M. (2020). Archaeometry: an overview. *Scientific Culture*, *6*(1), pp. 49-99.
Łucejko, J. J., Zborowska, M., Modugno, F., Colombini, M.P. and Prądzyński, W. (2012) Analytical pyrolysis vs. classical wet chemical analysis to assess the decay of archaeological waterlogged wood. *Analytica chimica acta* 745, pp. 70-77.
Łucejko, J. J., Modugno, F., Ribechini, E., Tamburini, D. and Colombini, M. P. (2015) Analytical instrumental techniques to study archaeological wood degradation. *Applied Spectroscopy Reviews* 50(7), pp. 584-625.
Macchioni, N., Pecoraro, E. and Pizzo, B. (2018) The measurement of maximum water content (MWC) on waterlogged archaeological wood: a comparison between three different methodologies. *Journal of Cultural Heritage* 30, pp. 51–56.
Macchioni, N., Pizzo, B., Capretti, C. and Giachi, G. (2012) How an integrated diagnostic approach can help in a correct evaluation of the state of preservation of waterlogged archaeological wooden artefacts. *Journal of archaeological science* 39(10), pp. 3255–3263.
McLean, J. P., Jin, G., Brennan, M., Nieuwoudt, M. K. and Harris, P. J. (2014) Using NIR and ATR-FTIR spectroscopy to rapidly detect compression wood in Pinus radiata. *Canadian Journal of Forest Research* 44(7), pp. 820-830.
Moosavinejad, S. M., Madhoushi, M., Vakili, M. and Rasouli, D. (2019) Evaluation of degradation in chemical compounds of wood in historical buildings using FT-IR and FT-Raman vibrational spectroscopy. Maderas. *Ciencia y tecnología* 21(3), pp. 381-39.
Müller, G., Schöpper, C., Vos, H., Kharazipour, A. and Polle, A. (2009) FTIR-ATR spectroscopic analyses of changes in wood properties during particle-and fibreboard production of hard-and softwood trees. *BioResources* 4(1), pp. 49-71.
Naumann, A., Peddireddi, S., Kües, U. and Polle, A. (2007) Fourier Transform Infrared Microscopy in Wood Analysis. *Wood production, wood technology, and biotechnological impacts*, pp. 179-196.
Ogilvie, T. M. A. (2000) *Water in archaeological wood: a critical appraisal of some diagnostic tools for degradation assessment*. Doctoral dissertation, Durham University.
Oron, A., Liphschitz, N., Held, B. W., Galili, E., Klein, M., Linker, R. and Blanchette, R. A. (2016) Characterization of archaeological waterlogged wooden objects exposed on the hyper-saline Dead Sea shore. *Journal of Archaeological Science: Reports* 9, pp. 73-86.
Pandey, K. K. (1999) A study of chemical structure of soft and hardwood and wood polymers by FTIR spectroscopy. *Journal of Applied Polymer Science 71*(12), pp. 1969-1975.
Pandey, K. K. and Pitman, A. J. (2003) FTIR studies of the changes in wood chemistry following decay by brown-rot and white-rot fungi. *International biodeterioration & biodegradation* 52(3), pp. 151-160.
Pizzo, B., Alves, A., Macchioni, N., Alves, A., Giachi, G., Schwanninger, M. And Rodrigues, J. (2010b) Characterization of waterlogged wood by infrared spectroscopy. *Proceedings of the International Conference "Wood Science for Conservation of Cultural Heritage"*, Firenze: Firenze University Press, pp.236-241.
Pizzo, B., Giachi, G. and Fiorentino, L. (2010a) Evaluation of the applicability of conventional methods for the chemical characterization of waterlogged archaeological wood. *Archaeometry* 52.4, pp. 656-667.
Pizzo, B., Pecoraro, E. and Macchioni, N. (2013) A new method to quantitatively evaluate the chemical composition of waterlogged wood by means of attenuated total reflectance Fourier transform infrared (ATR FT-IR) measurements carried out on wet material. *Applied spectroscopy* 67(5), pp. 553-562.
Pizzo, B., Pecoraro, E., Alves, A., Macchioni, N. and Rodrigues, J. C. (2015) Quantitative evaluation by attenuated total reflectance infrared (ATR-FTIR) spectroscopy of the chemical composition of decayed wood preserved in waterlogged conditions. *Talanta* 131, pp. 14-20.
Pucetaite, M. (2012). *Archaeological wood from the Swedish warship Vasa studied by infrared microscopy*. Master's thesis, Lund University.
Rashid, T., Kait, C. F. and Murugesan, T. (2016) A "Fourier Transformed infrared" compound study of lignin recovered from a formic acid process. *Procedia engineering* 148, pp. 1312-1319.
Rodgers, B. A. (2004) *The archaeologist's manual for conservation: a guide to non-toxic, minimal intervention artifact stabilization*. Springer Science & Business Media, (2004).
Salanti, A., Zoia, L., Tolppa, E. L., Giachi, G. and Orlandi, M. (2010) Characterization of waterlogged wood by NMR and GPC techniques. *Microchemical journal* 95(2), pp. 345-352.

Shearer, G. L. (1990) *An evaluation of Fourier transform infrared spectroscopy for the characterisation of organic compounds in art and archaeology*. Doctoral dissertation, University College London.

Shi, J., Xing, D. and Lia, J. (2012) FTIR studies of the changes in wood chemistry from wood forming tissue under inclined treatment. *Energy Procedia 16*, pp. 758-762.

Stevanic, J. S. and Salmén, L. (2009) Orientation of the wood polymers in the cell wall of spruce wood fibres. *Holzforschung* 63, pp. 497–503.

Traoré, M., Kaal, J. and Cortizas, A. M. (2016) Application of FTIR spectroscopy to the characterization of archeological wood. *Spectrochimica Acta Part A: Molecular and Biomolecular Spectroscopy* 153, pp. 63-70.

Traoré, M., Kaal, J. and Cortizas, A. M. (2018) Differentiation between pine woods according to species and growing location using FTIR-ATR. *Wood science and technology* 52(2), pp. 487-504.

Viet, D. Q. (2017) Study on characteristics of acacia wood by FTIR and thermogrametric analysis. *Vietnam Journal of Chemistry* 55(2), 259.

Zborowska, M., Stachowiak-Wencek, A., Waliszewska, B. and Prądzyński, W. (2016) Colourimetric and FT-IR ATR spectroscopy studies of degradative effects of ultraviolet light on the surface of exotic ipe (Tabebuia sp.) wood. Cellulose Chemistry and Technology 50, pp. 71-76.